

Contents lists available at [ScienceDirect](https://www.sciencedirect.com)

International Journal for Parasitology: Drugs and Drug Resistance

journal homepage: www.elsevier.com/locate/ijpddr

Novel acyl carbamates and acyl / diacyl ureas show *in vitro* efficacy against *Toxoplasma gondii* and *Cryptosporidium parvum*

Kun Li^{a,1,2}, Gregory M. Grooms^{b,2}, Shahbaz M. Khan^a, Anolan Garcia Hernandez^b,
William H. Witola^{a,**}, Jozef Stec^{b,c,*}

^a Department of Pathobiology, College of Veterinary Medicine, University of Illinois at Urbana-Champaign, Urbana, IL 61802, USA

^b Chicago State University, College of Pharmacy, Department of Pharmaceutical Sciences, 9501 S. King Drive, Chicago, IL 60628, USA

^c Marshall B. Ketchum University, College of Pharmacy, Department of Pharmaceutical Sciences, 2575 Yorba Linda Blvd., Fullerton, CA 82831, USA

ARTICLE INFO

Keywords:

Toxoplasma gondii
Cryptosporidium parvum
Acyl carbamate
Acyl urea
Diacyl urea
Drug discovery

ABSTRACT

Toxoplasma gondii and *Cryptosporidium parvum* are protozoan parasites that are highly prevalent and opportunistically infect humans worldwide, but for which completely effective and safe medications are lacking. Herein, we synthesized a series of novel small molecules bearing the diacyl urea scaffold and related structures, and screened them for *in vitro* cytotoxicity and antiparasitic activity against *T. gondii* and *C. parvum*. We identified one compound (GMG-1-09), and four compounds (JS-1-09, JS-2-20, JS-2-35 and JS-2-49) with efficacy against *C. parvum* and *T. gondii*, respectively, at low micromolar concentrations and showed appreciable selectivity in human host cells. Among the four compounds with efficacy against *T. gondii*, JS-1-09 representing the diacyl urea scaffold was the most effective, with an anti-*Toxoplasma* IC₅₀ concentration (1.21 μM) that was nearly 53-fold lower than its cytotoxicity IC₅₀ concentration, indicating that this compound has a good selectivity index. The other three compounds (JS-2-20, JS-2-35 and JS-2-49) were structurally more divergent from JS-1-09 as they represent the acyl urea and acyl carbamate scaffold. This appeared to correlate with their anti-*Toxoplasma* activity, suggesting that these compounds' potency can likely be enhanced by selective structural modifications. One compound, GMG-1-09 representing acyl carbamate scaffold, depicted *in vitro* efficacy against *C. parvum* with an IC₅₀ concentration (32.24 μM) that was 14-fold lower than its cytotoxicity IC₅₀ concentration in a human intestinal cell line. Together, our studies unveil a series of novel synthetic acyl/diacyl urea and acyl carbamate scaffold-based small molecule compounds with micromolar activity against *T. gondii* and *C. parvum* that can be explored further for the development of the much-needed novel anti-protozoal drugs.

1. Introduction

Toxoplasma gondii and *Cryptosporidium parvum* are apicomplexan protozoan zoonotic parasites that are highly prevalent and are common opportunistic infections of humans worldwide (Chalmers et al., 2014; Kochanowsky and Koshy, 2018). The global seroprevalence (measured by IgG levels) of *T. gondii* varies greatly by country and region (Furtado et al., 2011), and is predominantly impacted by environmental and socio-cultural factors (Mboera et al., 2019). It is estimated that 11% of

the US population is infected with this parasite (Centers for Disease Control and Prevention (CDC), 2020a), and the infection is considered to be one of the five neglected parasitic infections targeted by CDC for public health action in the U.S.A (Centers for Disease Control and Prevention (CDC), 2020b). In immunocompromised individuals, and in congenitally infected children, *T. gondii* can cause serious illnesses, including ocular and neurologic illnesses, and systemic spread of the parasite leading to vital organ failure (Alday and Doggett, 2017). The current gold standard for the treatment of *T. gondii* infections involves a

* Corresponding author. Marshall B. Ketchum University, College of Pharmacy, Department of Pharmaceutical Sciences, 2575 Yorba Linda Blvd., Fullerton, CA 82831, USA.

** Corresponding author. Department of Pathobiology, College of Veterinary Medicine, University of Illinois at Urbana-Champaign, Urbana, IL 61802, USA
E-mail addresses: whwit35@illinois.edu (W.H. Witola), jstec@ketchum.edu (J. Stec).

¹ Present address: Institute of Traditional Chinese Veterinary Medicine, College of Veterinary Medicine, Nanjing Agricultural University, Nanjing 210095, PR China.

² These authors contributed equally.

<https://doi.org/10.1016/j.ijpddr.2020.08.006>

Received 4 June 2020; Received in revised form 7 August 2020; Accepted 19 August 2020

Available online 25 August 2020

2211-3207/© 2020 The Authors. Published by Elsevier Ltd on behalf of Australian Society for Parasitology. This is an open access article under the CC BY-NC-ND

license (<http://creativecommons.org/licenses/by-nc-nd/4.0/>).

combination of pyrimethamine and sulfadiazine. Other treatment regimens include a combination of trimethoprim and sulfamethoxazole, and atovaquone alone or in combination with sulfadiazine. However, all these treatment regimens are limited by hypersensitivity reactions, gastrointestinal and hematologic toxicities, and are ineffective against the encysted stage of the parasite. On the other hand, *C. parvum* is a major cause of diarrheal diseases in children under the age of two and in immunocompromised individuals, resulting in significant morbidity and mortality especially in poor-resource areas of developing countries (Checkley et al., 2015). The only FDA-approved anti-*Cryptosporidium* drug in humans, nitazoxanide, is ineffective in those individuals most at risk for morbidity and mortality due to *Cryptosporidium* infections, including malnourished young children and immunocompromised individuals (Abubakar et al., 2007). Coupled with the lack of human vaccines against *Toxoplasma* and *Cryptosporidium*, there is an urgent need to develop safe and effective therapeutic agents against these devastating parasites.

Within the last two decades, medicinal chemistry research efforts have resulted in discovering and developing diverse lead compounds with excellent activity against *T. gondii* (Alday and Doggett, 2017). The majority of the lead compounds were identified through phenotypic screening of small molecule libraries. More recently, analogs of various natural products such as thiolactomycin (Martins-Duarte et al., 2009), trypanthrin (Krivogorsky et al., 2013), arctigenin (Zhang et al., 2018), (+)-usnic and ursolic acids (Guo et al., 2019; Luan et al., 2019), and dihydroartemisinin (Deng et al., 2020) have been reported to be effective against *T. gondii*. More interestingly, some compounds were initially discovered as antiparasitic agents and subsequently were shown to be also active against *T. gondii*. Examples of such repurposed compounds include the imide QQ-437 (Fomovska et al., 2012), spiroindolone NITD609 (Zhou et al., 2014), and piperazine acetamide (Boyom et al., 2014) (S1 Fig.).

In the present study, we synthesized a series of novel small molecule compounds based on the scaffold of acyl/diacyl urea and acyl carbamate, and screened them for *in vitro* antiparasitic activity against *T. gondii* and *C. parvum*. We identified one compound, and four compounds with activity at low micromolar concentrations against *C. parvum* and *T. gondii*, respectively, that were nontoxic to mammalian host cells. Our results suggest that the acyl/diacyl urea and acyl carbamate scaffolds can potentially be used to derive new antiparasitic drug candidates.

2. Materials and methods

2.1. Chemistry

2.1.1. General information

All standard reagents were purchased from Sigma-Aldrich and Fisher Scientific. Anhydrous toluene (PhCH₃) was purchased from Sigma-Aldrich whereas anhydrous dichloromethane (CH₂Cl₂) was obtained by distillation over calcium hydride. ¹H NMR and ¹³C NMR spectra were recorded on JEOL spectrometer at 400 and 100 MHz, respectively. NMR spectra were reprocessed by ACD/NMR Processor Academic Edition version 12.01. Standard abbreviations indicating multiplicity were used as follows: s = singlet, d = doublet, dd = doublet of doublets, t = triplet, q = quadruplet, m = multiplet, and br = broad. HR-MS experiments were performed on Agilent 6224 ToF-MS instrument. TLC was performed on Merck 60 F254 silica gel plates. Flash chromatography was performed using a Biotage - Isolera™ system with pre-packed silica columns (Biotage FLSH SNAP CRT SI 10, 25, or 50 g). All tested compounds were ≥95% pure as determined by ¹H NMR and analytical HPLC: Shimadzu LC-2010 all-in-one system equipped with auto-injector and UV/Vis detector (variable wavelength). The system was controlled by LabSolutions™ (Shimadzu) running under Windows 7. The used method: flow rate = 1.4 mL/min, gradient elution over 20 min, from 30% MeOH/H₂O to 100% MeOH with 0.05% TFA with Phenomenex Synergi 4 μm Hydro-

RP 80A column, 150 mm.

2.1.2. General procedure for the synthesis of the target compounds 1-21

The appropriate starting material (I), which was usually a primary amide (1.0 mmol, 1.0 eq), was placed in a Schlenk Kjeldahl reaction flask and the flask was evacuated/Argon re-filled three times. Subsequently, anhydrous dichloromethane (25 mL) was added and the mixture was stirred at room temperature (RT) for 5 min before dropwise addition of oxalyl chloride (3.0 mmol, 3.0 eq). The reaction mixture was then stirred at reflux for 2.5–3.0 h before cooling to RT and the solvent was removed under reduced pressure. Subsequently 1.1–1.25 mmol (1.1–1.25 eq) of the appropriate nucleophile (III) was rapidly added and the flask was evacuated/Argon re-filled before dry toluene (12 mL) was added. The reaction mixture was then stirred at reflux for 2.5–3 h before cooling to RT and concentration on rotavapor. Compounds 1, 3, and 4 were isolated through suction filtration as solids in high purity (>95%), therefore they were used without further purification. Compounds 2 and 11 were isolated as solids but the crude materials were purified by crystallization from methanol and hexane:ethyl acetate, respectively. All other compounds were purified by automated flash chromatography on silica with hexane-ethyl acetate as the eluent.

2.1.3. Analytical data of the synthesized compounds

- 1, N'-Carbonyldibenzamide (JS-1-07):** Milky-white solid, 240 mg (89%). Analytical data for this compound were reported previously (Garcia Hernandez et al., 2017).
- N, N'-Carbonylbis(2-nitrobenzamide) (JS-1-11):** White powder, 250 mg (70%). Analytical data for this compound were reported previously (Garcia Hernandez et al., 2017).
- N, N'-Carbonylbis(2-methoxybenzamide) (JS-1-09):** Grey powder, 288 mg (88%). Analytical data for this compound were reported previously (Garcia Hernandez et al., 2017).
- N¹N²-Dibenzoyloxalohydrazide (JS-1-37):** Pale yellow solid, 251 mg (77%). Analytical data for this compound were reported previously (Garcia Hernandez et al., 2017).
- 2,3,4-Trifluoro-N-(((1R,2R,3R,5S)-2,6,6-trimethylbicyclo[3.1.1]heptan-3-yl)carbamoyl)-benzamide (JS-2-11):** White solid, 210 mg (59%).

¹H NMR (400 MHz, DMSO-*d*₆) δ ppm 10.8 (br s, 1H), 8.23 (m, *J* = 8.2 Hz, 1H), 7.51 (m, 1H), 7.40 (m, 1H), 4.07 (m, 1H), 2.42–2.31 (m, 2H), 1.90–1.86 (m, 2H), 1.76 (td, *J* = 5.7, 1.4 Hz, 1H), 1.58 (ddd, *J* = 13.7, 6.4, 2.3 Hz, 1H), 1.17 (br s, 3H), 1.04 (d, *J* = 7.3 Hz, 3H), 0.97 (br s, 3H), 0.95 (d, *J* = 10.8 Hz, 1H).

¹³C NMR (100 MHz, DMSO-*d*₆) δ ppm 164.6 (C), 152.8 (C), 152.6 (C, ddd, *J* = 252.1, 9.6, 2.9 Hz), 149.0 (C, ddd, *J* = 250.0, 11.0, 3.4 Hz), 139.4 (C, dt, *J* = 249.7, 15.6 Hz), 125.3 (CH, dd, *J* = 7.7, 3.8 Hz), 121.4 (C, dd, *J* = 10.5, 2.9 Hz), 113.5 (CH, dd, *J* = 17.7, 3.4 Hz), 48.4 (CH), 47.7 (CH), 45.5 (CH), 41.5 (CH), 38.6 (C), 37.0 (CH₂), 34.9 (CH₂), 28.4 (CH₃), 23.7 (CH₃), 21.1 (CH₃).

HRMS (TOF): *m/z* [M]⁺ calculated for C₁₈H₂₁F₃N₂O₂: 354.1555, found: 354.1544.

- N-((Adamantan-1-yl)carbamoyl)-2,3,4-trifluorobenzamide (JS-2-14):** White solid, 173 mg (49%).

¹H NMR (400 MHz, DMSO-*d*₆) δ ppm 10.65 (s, 1H), 8.16 (s, 1H), 7.48 (m, 1H), 7.39 (m, 1H), 2.01 (s, 3H), 1.94–1.93 (m, 6H), 1.60 (s, 6H).

¹³C NMR (100 MHz, DMSO-*d*₆) δ ppm 164.9 (C), 152.2 (C, ddd, *J* = 255.9, 10.1, 2.4 Hz), 151.2 (C), 148.9 (C, ddd, *J* = 254.5, 11.0, 3.4 Hz), 139.4 (C, dt, *J* = 249.2, 15.6 Hz), 125.3 (CH, dd, *J* = 7.7, 2.1 Hz), 121.4 (C, dd, *J* = 11.0, 2.4 Hz), 113.5 (CH, dd, *J* = 17.7, 3.4 Hz), 51.1 (C), 41.6 (3CH₂), 36.3 (3CH₂), 29.3 (3CH₃).

HRMS (TOF): *m/z* [M]⁺ calculated for C₁₈H₁₉F₃N₂O₂: 352.1399, found: 352.1397.

7. ***N*-((Adamantan-2-yl)carbamoyl)-2,3,4-trifluorobenzamide (JS-2-34)**: White solid, 223 mg (63%).

¹H NMR (400 MHz, DMSO-*d*₆) δ ppm 10.89 (s, 1H), 8.73 (d, *J* = 7.8 Hz, 1H), 7.52 (m, 1H), 7.41 (m, 1H), 3.86 (d, *J* = 7.8 Hz, 1H), 1.86–1.68 (m, 12H), 1.59 (d, *J* = 12.4 Hz, 2H).

¹³C NMR (100 MHz, DMSO-*d*₆) δ ppm 165.1 (C), 152.6 (C, ddd, *J* = 251.6, 9.6, 2.9 Hz), 152.2 (C), 149.0 (C, ddd, *J* = 254.7, 10.8, 3.6 Hz), 139.4 (C, dt, *J* = 248.9, 16.3 Hz), 125.4 (CH, dd, *J* = 5.3, 3.6 Hz), 121.3 (C, dd, *J* = 10.5, 3.8 Hz), 113.5 (CH, dd, *J* = 17.7, 3.4 Hz), 53.7 (CH), 37.4 (CH₂), 36.9 (2CH₂), 32.0 (2CH), 31.9 (2CH₂), 27.1 (CH), 27.0 (CH).

HRMS (TOF): *m/z* [M]⁺ calculated for C₁₈H₁₉F₃N₂O₂: 352.1399, found: 352.1406.

8. ***N*-((Cyclooctylcarbamoyl)-2,3,4-trifluorobenzamide (JS-2-36)**: White powder, 280 mg (85%).

¹H NMR (400 MHz, DMSO-*d*₆) δ ppm 10.79 (br s, 1H), 8.25 (d, *J* = 7.3 Hz, 1H), 7.49 (m, 1H), 7.40 (m, 1H), 3.78 (qt, *J* = 8.2, 4.1 Hz, 1H), 1.79–1.73 (m, 2H), 1.59–1.45 (m, 12H).

¹³C NMR (100 MHz, DMSO-*d*₆) δ ppm 164.7 (C), 152.6 (C, ddd, *J* = 252.1, 9.6, 2.8 Hz), 152.1 (C), 149.0 (C, ddd, *J* = 254.7, 10.8, 3.6 Hz), 139.4 (C, dt, *J* = 249.8, 15.8, 15.3 Hz), 125.4 (CH, dd, *J* = 8.6, 5.8 Hz), 121.4 (C, dd, *J* = 11.0, 2.4 Hz), 113.5 (CH, dd, *J* = 17.7, 3.4 Hz), 49.8 (CH), 31.8 (2CH₂), 27.4 (2CH₂), 25.3 (CH₂), 23.5 (2CH₂).

HRMS (TOF): *m/z* [M]⁺ calculated for C₁₆H₁₉F₃N₂O₂: 328.1399, found: 328.1408.

9. ***(E)*-*N*-((3,7-Dimethylocta-2,6-dien-1-yl)carbamoyl)-2,3,4-trifluorobenzamide (JS-2-20)**: White solid, 122 mg (34%). Analytical data for this compound were reported previously (Garcia Hernandez et al., 2017).

10. **2,4-Dichloro-*N*-(((1*R*,2*R*,3*R*,5*S*)-2,6,6-trimethylbicyclo [3.1.1]heptan-3-yl)carbamoyl)benzamide (JS-2-10)**: White solid, 244 mg (66%).

¹H NMR (400 MHz, DMSO-*d*₆) δ ppm 10.84 (br s, 1H), 8.22 (br s, 1H), 7.70 (d, *J* = 2.3, 1H), 7.56 (d, *J* = 8.2, 1H), 7.47 (dd, *J* = 8.2, 1.8 Hz, 1H), 4.06 (m, 1H), 2.41–2.31 (m, 2H), 1.90–1.85 (m, 2H), 1.76 (td, *J* = 5.7, 1.4 Hz, 1H), 1.58 (ddd, *J* = 13.7, 6.2, 2.1 Hz, 1H), 1.17 (br s, 3H), 1.04 (d, *J* = 7.3 Hz, 3H), 0.97 (s, 3H), 0.95 (d, *J* = 9.6 Hz, 1H).

¹³C NMR (100 MHz, DMSO-*d*₆) δ ppm 167.9 (C), 152.9 (C), 136.0 (C), 134.4 (C), 131.6 (C), 130.9 (CH), 129.7 (CH), 127.9 (CH), 48.3 (CH), 47.7 (CH), 45.6 (CH), 41.5 (CH), 38.6 (C), 37.1 (CH₂), 34.9 (CH₂), 28.4 (CH₃), 23.7 (CH₃), 21.2 (CH₃).

HRMS (TOF): *m/z* [M]⁺ calculated for C₁₈H₂₂Cl₂N₂O₂: 368.1058, found: 368.1054.

11. **3-Iodo-*N*-(((1*R*,2*R*,3*R*,5*S*)-2,6,6-trimethylbicyclo [3.1.1]heptan-3-yl)carbamoyl)-benzamide (JS-2-16)**: White powder, 298 mg (70%).

¹H NMR (400 MHz, DMSO-*d*₆) δ ppm 10.25 (br s, 1H), 8.55 (d, *J* = 8.2 Hz, 1H), 8.25 (t, *J* = 1.8 Hz, 1H), 7.93–7.89 (m, 2H), 7.26 (t, *J* = 7.8 Hz, 1H), 4.08 (m, 1H), 2.49–2.32 (m, 2H), 1.90–1.82 (m, 2H), 1.77 (td, *J* = 6.0, 1.4 Hz, 1H), 1.57 (ddd, *J* = 14.0, 6.2, 2.3 Hz, 1H), 1.17 (br s, 3H), 1.04 (d, *J* = 6.9 Hz, 3H), 0.98 (br s, 3H), 0.93 (d, *J* = 10.1 Hz, 1H).

¹³C NMR (100 MHz, DMSO-*d*₆) δ ppm 167.5 (C), 153.4 (C), 141.6 (CH), 137.0 (CH), 135.2 (CH), 131.1 (CH), 128.0 (CH), 95.2 (C), 48.2 (C), 47.7 (CH), 45.7 (CH), 41.6 (CH), 40.3 (C), 37.2 (CH₂), 35.0 (CH₂), 28.4 (CH₃), 23.7 (CH₃), 21.2 (CH₃).

HRMS (TOF): *m/z* [M]⁺ calculated for C₁₈H₂₃I₂N₂O₂: 426.0804, found: 426.0801.

12. **3-Bromo-*N*-(((1*R*,2*R*,3*R*,5*S*)-2,6,6-trimethylbicyclo [3.1.1]heptan-3-yl)carbamoyl)-benzamide (JS-2-17)**: White solid, 250 mg (66%).

¹H NMR (400 MHz, DMSO-*d*₆) δ ppm 10.74 (s, 1H), 8.54 (d, *J* = 8.2 Hz, 1H), 8.10 (t, *J* = 1.6 Hz, 1H), 7.89 (dd, *J* = 7.8, 0.9 Hz, 1H), 7.77 (dt, *J* = 6.9, 0.9 Hz, 1H), 7.43 (t, *J* = 8.0 Hz, 1H), 4.09 (dt, *J* = 15.9, 7.8 Hz, 1H), 2.48–2.32 (m, 2H), 1.94–1.84 (m, 2H), 1.77 (t, *J* = 5.3 Hz, 1H), 1.58 (ddd, *J* = 13.9, 6.3, 1.8 Hz, 1H), 1.18 (br s, 3H), 1.05 (d, *J* = 6.9 Hz, 3H), 0.98 (s, 3H), 0.94 (d, *J* = 9.6 Hz, 1H).

¹³C NMR (100 MHz, DMSO-*d*₆) δ ppm 167.5 (C), 153.4 (C), 135.9 (CH), 135.3 (CH), 131.3 (CH), 131.2 (CH), 127.7 (CH), 122.2 (C), 48.3 (C), 47.7 (CH), 45.7 (CH), 41.6 (CH), 38.5 (C), 37.2 (CH₂), 35.0 (CH₂), 28.4 (CH₃), 23.7 (CH₃), 21.2 (CH₃).

HRMS (TOF): *m/z* [M]⁺ calculated for C₁₈H₂₃BrN₂O₂: 378.0943, found: 378.0942.

13. ***N*-(((1*R*,2*R*,3*R*,5*S*)-2,6,6-Trimethylbicyclo [3.1.1] heptan-3-yl)carbamoyl)adamantane-1-carboxamide (AGH-1-09)**: White solid, 208 mg (58%).

¹H NMR (400 MHz, CDCl₃) δ ppm 8.55 (d, *J* = 8.2 Hz, 1H), 8.19 (br s, 1H), 4.22–4.14 (m, 1H), 2.61–2.54 (m, 1H), 2.41–2.35 (m, 1H), 2.06 (s, 3H), 1.95–1.60 (m, 16H), 1.20 (s, 3H), 1.11 (d, *J* = 7.3 Hz, 3H), 1.01 (s, 3H), 0.90 (d, *J* = 9.6 Hz, 1H).

¹³C NMR (100 MHz, CDCl₃) δ ppm 179.6 (C), 153.7 (C), 48.5 (CH), 47.8 (CH), 46.1 (CH), 41.8 (C), 41.6 (CH), 38.6 (3CH₂), 38.5 (C), 37.2 (CH₂), 36.3 (3CH₂), 35.1 (CH₂), 28.1 (CH₃), 28.0 (3CH), 23.5 (CH₃), 20.9 (CH₃).

HRMS (TOF): *m/z* [M]⁺ calculated for C₂₂H₃₄N₂O₂: 358.2620, found: 358.2616.

14. ***N*-((Adamantan-2-yl)carbamoyl)adamantane-1-carboxamide (GMG-1-11)**: White powder, 212 mg (60%). Analytical data for this compound were reported previously (Garcia Hernandez et al., 2017).

15. ***N*-(((E)-3,7-Dimethylocta-2,6-dien-1-yl)carbamoyl)adamantane-1-carboxamide (JS-2-21)**: White solid, 302 mg (84%).

¹H NMR (400 MHz, DMSO-*d*₆) δ ppm 9.71 (br s, 1H), 8.44 (t, *J* = 5.3 Hz, 1H), 5.14 (t, *J* = 6.6 Hz, 1H), 5.01 (td, *J* = 6.2, 1.4 Hz, 1H), 3.70 (t, *J* = 6.2 Hz, 2H), 2.02–1.97 (m, 2H), 1.93–1.91 (m, 5H), 1.78–1.77 (m, 6H), 1.63–1.59 (m, 12H), 1.51 (br s, 3H).

¹³C NMR (100 MHz, DMSO-*d*₆) δ ppm 180.0 (C), 154.2 (C), 138.4 (C), 131.5 (C), 124.4 (CH), 121.5 (CH), 41.7 (C), 39.4 (CH₂), 37.8 (3CH₂), 37.2 (CH₂), 36.2 (3CH₂), 28.0 (3CH), 26.4 (CH₃), 26.0 (CH₃), 18.1 (CH₃), 16.5 (CH₃).

HRMS (TOF): *m/z* [M]⁺ calculated for C₂₂H₃₄N₂O₂: 358.2620, found: 358.2619.

16. **Adamantan-1-yl (2,3,4-trifluorobenzoyl)carbamate (JS-2-49)**: White solid, 285 mg (81%).

¹H NMR (400 MHz, DMSO-*d*₆) δ ppm 10.98 (s, 1H), 7.43–7.33 (m, 2H), 2.09 (br s, 3H), 2.00 (br s, 6H), 1.57 (br s, 6H).

¹³C NMR (100 MHz, DMSO-*d*₆) δ ppm 163.2 (C), 152.3 (C, ddd, *J* = 251.6, 9.6, 2.9 Hz), 150.0 (C), 148.6 (C, ddd, *J* = 252.8, 10.8, 3.1 Hz), 139.2 (C, dt, *J* = 249.5, 15.6 Hz), 125.1 (CH, dd, *J* = 8.6, 3.8 Hz), 122.5 (C, dd, *J* = 12.5, 2.9 Hz), 113.5 (CH, dd, *J* = 17.3, 2.9 Hz), 81.7 (C), 41.2 (3CH₂), 36.0 (3CH₂), 30.7 (3CH).

HRMS (TOF): *m/z* [M]⁺ calculated for C₁₈H₁₈F₃NO₃: 353.1239, found: 353.1242.

17. **Adamantan-2-yl (2,3,4-trifluorobenzoyl)carbamate (JS-2-35)**: White solid, 345 mg (98%).

¹H NMR (400 MHz, DMSO-*d*₆) δ ppm 11.18 (s, 1H), 7.48–7.36 (m, 2H), 4.76 (t, *J* = 3.2 Hz, 1H), 1.93–1.90 (m, 4H), 1.78–1.65 (m, 8H), 1.47 (d, *J* = 12.4 Hz, 2H).

¹³C NMR (100 MHz, DMSO-*d*₆) δ ppm 163.0 (C), 152.4 (C, ddd, *J* = 251.7, 9.8, 2.6 Hz), 151.3 (C), 148.7 (C, ddd, *J* = 253.0, 11.0, 3.4 Hz), 139.2 (C, dt, *J* = 249.5, 15.6 Hz), 125.2 (CH, dd, *J* = 8.2, 4.3 Hz), 122.3 (C, dd, *J* = 12.5, 2.3 Hz), 113.5 (CH, dd, *J* = 17.7, 3.4 Hz), 78.6 (CH), 37.2 (CH₂), 36.0 (2CH₂), 31.7 (2CH), 31.5 (2CH₂), 27.0 (CH), 26.8 (CH).

HRMS (TOF): *m/z* [M]⁺ calculated for C₁₈H₁₈F₃NO₃: 353.1239, found: 353.1239.

18. (E)-3,7-Dimethylocta-2,6-dien-1-yl (2,3,4-trifluorobenzoyl) carbamate (AGH-1-08): White solid, 213 mg (60%).

¹H NMR (400 MHz, CDCl₃) δ ppm 11.23 (s, 1H), 7.45–7.34 (m, 2H), 5.27 (m, *J* = 7.2, 1.1 Hz, 1H), 5.02 (m, 1H), 4.58 (d, *J* = 7.3 Hz, 2H), 2.04–1.94 (m, 4H), 1.63 (d, *J* = 0.9 Hz, 3H), 1.59 (d, *J* = 0.9 Hz, 3H), 1.52 (br s, 3H).

¹³C NMR (100 MHz, CDCl₃) δ ppm 162.9 (C), 152.4 (CF, ddd, *J* = 254.0, 10.5, 2.9 Hz), 151.8 (C), 148.8 (CF, ddd, *J* = 254.0, 10.5, 2.9 Hz), 143.0 (C), 139.2 (CF, dt, *J* = 249.2, 15.8 Hz), 131.7 (C), 125.2 (CH, dd, *J* = 8.6, 3.8 Hz), 124.2 (CH), 122.2 (C, dd, *J* = 11.5, 2.9 Hz), 118.4 (CH), 113.5 (C, dd, *J* = 17.8, 3.3 Hz), 62.5 (OCH₂), 39.4 (CH₂), 26.2 (CH₂), 26.0 (CH₃), 18.1 (CH₃), 16.7 (CH₃).

HRMS (TOF): *m/z* [M]⁺ calculated for C₁₈H₂₀F₃NO₃: 355.1395, found: 355.1399.

19. (Z)-3,7-Dimethylocta-2,6-dien-1-yl (2,3,4-trifluorobenzoyl) carbamate (GMG-1-10): White solid, 161 mg (45%).

¹H NMR (400 MHz, CDCl₃) δ ppm 8.22 (d, *J* = 9.6 Hz, 1H), 7.78 (m, 1H), 7.12 (m, 1H), 5.38 (t, *J* = 7.3 Hz, 1H), 5.07 (m, 1H), 4.70 (d, *J* = 7.3 Hz, 2H), 2.15–2.03 (m, 4H), 1.77 (br s, 3H), 1.67 (br s, 3H), 1.59 (br s, 3H).

¹³C NMR (100 MHz, CDCl₃) δ ppm 159.9 (C), 154.1 (CF, ddd, *J* = 258.8, 9.6, 2.8 Hz), 150.4 (C), 149.9 (CF, ddd, *J* = 252.1, 11.5, 3.8 Hz), 144.3 (C), 139.8 (CF, dt, *J* = 254.0, 16.3 Hz), 132.5 (C), 126.2 (CH, dd, *J* = 6.7, 1.9 Hz), 123.4 (CH), 118.3 (C), 118.1 (CH), 113.4 (CH, dd, *J* = 17.7, 3.3), 63.2 (CH₂), 32.3 (CH₂), 26.7 (CH₂), 25.8 (CH₃), 23.6 (CH₃), 17.7 (CH₃).

HRMS (TOF): *m/z* [M]⁺ calculated for C₁₈H₂₀F₃NO₃: 355.1395, found: 355.1394.

20. (E)-3,7-Dimethylocta-2,6-dien-1-yl (adamantane-1-carbonyl) carbamate (GMG-1-08): White solid, 113 mg (31%).

¹H NMR (400 MHz, CDCl₃) δ ppm 7.55 (s, 1H), 5.35 (td, *J* = 7.2, 1.1 Hz, 1H), 5.05 (td, *J* = 6.2, 1.4 Hz, 1H), 4.67 (d, *J* = 7.3 Hz, 2H), 2.11–2.02 (m, 7 H), 1.85 (br s, 6H), 1.75–1.62 (m, 6H), 1.70 (s, 3H), 1.66 (s, 3H), 1.58 (s, 3H).

¹³C NMR (100 MHz, CDCl₃) δ ppm 175.1 (C), 151.1 (C), 143.6 (C), 132.0 (C), 123.7 (CH), 117.5 (CH), 62.9 (OCH₂), 42.2 (C), 39.6 (CH₂), 38.8 (3CH₂), 36.3 (3CH₂), 27.9 (3CH), 26.3 (CH₂), 25.8 (CH₃), 17.8 (CH₃), 16.6 (CH₃).

HRMS (TOF): *m/z* [M]⁺ calculated for C₂₂H₃₃NO₃: 359.2460, found: 359.2471.

21. (Z)-3,7-Dimethylocta-2,6-dien-1-yl (adamantane-1-carbonyl) carbamate (GMG-1-09): White solid, 103 mg (29%).

¹H NMR (400 MHz, CDCl₃) δ ppm 7.53 (s, 1H), 5.36 (t, *J* = 7.3 Hz, 1H), 5.06 (t, *J* = 6.9 Hz, 1H), 4.64 (d, *J* = 7.3 Hz, 2H), 2.15–2.05 (m, 7H), 1.85 (br s, 6H), 1.75 (s, 3H), 1.75–1.59 (m, 6H), 1.66 (s, 3H), 1.59 (m, 3H).

¹³C NMR (100 MHz, CDCl₃) δ ppm 175.1 (C), 151.0 (C), 143.8 (C), 132.4 (C), 123.5 (CH), 118.5 (CH), 62.6 (CH₂), 42.2 (C), 38.8 (3CH₂), 3

6.3 (3CH₂), 32.3 (CH₂), 27.9 (3CH), 26.7 (CH₂), 25.8 (CH₃), 23.6 (CH₃), 17.8 (CH₃).

HRMS (TOF): *m/z* [M]⁺ calculated for C₂₂H₃₃NO₃: 359.2460, found: 359.2471.

2.2. Biology

2.2.1. Parasites

The AUCP-1 isolate of *C. parvum* and the Type 1 RH strain of *T. gondii* were used in the experiments. *C. parvum* parasites were propagated in male Holstein calves in accordance with the guidelines of protocol number 18108 approved by the University of Illinois at Urbana-Champaign, USA. *C. parvum* oocysts were extracted from fresh calf feces by sequential sieve filtration, Sheather's sugar flotation, and discontinuous sucrose density gradient centrifugation, essentially as previously described (Arrowood and Sterling, 1987; Current et al., 1992). Purified oocysts were stored in phosphate-buffered saline (PBS) at 4 °C and used within 3 months. *C. parvum* sporozoites excystation from oocysts was done essentially as previously reported (Kuhlenschmidt et al., 2016). Briefly, 500 μl of 40% commercial laundry bleach was added to 1 × 10⁸ *C. parvum* oocysts suspended in 500 μl of PBS, and incubated for 10 min at 4 °C, followed by four washes in PBS containing 1% (w/v) bovine serum albumin. The washed oocysts were resuspended in Hanks balanced salt solution and incubated for 60 min at 37 °C, followed by addition of an equal volume of warm 1.5% sodium tauracholate in Hanks balanced salt solution and further incubation for 60 min at 37 °C with occasional shaking. The excysted sporozoites were collected by centrifugation and resuspended in PBS. The excysted sporozoites were purified by passing the suspension through a sterile 5 μm syringe filter (Millex) and counted with a hemocytometer.

Tachyzoites of Type I RH strain of *T. gondii* engineered to constitutively express cytosolic yellow fluorescent protein (YFP) (Gubbels et al., 2003) were maintained in human foreskin fibroblasts (HFF) (American Type Culture Collection Item number: ATCC SCRC1041) cultured in Iscove's modified Dulbecco's medium supplemented with 10% (v/v) heat-inactivated fetal bovine serum, 1% (v/v) GlutaMAX, and 1% (v/v) penicillin-streptomycin-amphotericin B (Fungizone) (Life Technologies) at 37 °C with 5% CO₂. To extract *T. gondii* tachyzoites, the infected HFFs were suspended in medium and passed through a 25-gauge needle twice, followed by filtering through a 3-μm-pore-size filter to isolate the parasites from the cell debris. Isolated parasites were washed three times in PBS and enumerated using a hemocytometer.

2.2.2. Cytotoxicity assays

All compounds were first tested for cytotoxicity at a concentration of 40 μM in human ileocecal adenocarcinoma (HCT-8) cells (American Type Culture Collection Item number: CCL244) and HFF cells that were used for *in vitro* culture of *C. parvum* and *T. gondii*, respectively. Subsequently, compounds that were non-toxic at 40 μM, but had significant antiparasitic effect, were titrated (concentrations ranging from 0 to 700 μM) to derive their half maximal cytotoxicity concentrations (IC₅₀ values) in uninfected HCT-8 and HFF cells. Briefly, HCT-8 cells were cultured in 96-well plates in 200 μl of RPMI 1640 medium without phenol red (Life Technologies), but supplemented with 2 g/L of sodium bicarbonate, 2.5 g/L of glucose, 10% fetal bovine serum (FBS) (Gibco, USA), 1 × antibiotic-antimycotic (Gibco), and 1 × sodium pyruvate (Gibco). HFF cells were cultured in 96-well plates in 200 μl of Dulbecco's modified medium (without phenol red) supplemented with 10% (v/v) FBS, 1% (v/v) GlutaMAX, and 1% (v/v) penicillin-streptomycin-amphotericin B (Fungizone) (Life Technologies) at 37 °C with 5% CO₂. When the cells were confluent, old medium was replaced with fresh medium with or without the test compounds (40 μM final concentration) reconstituted in dimethyl sulfoxide (DMSO), molecular biology grade (Sigma Aldrich). The highest volume of compound added per well did not exceed 1% of the total culture volume in order to avoid DMSO toxicity to the cells. Control wells received equivalent volumes of DMSO without compound.

After 48 h of culture, 10 μ l of the cell proliferation reagent WST-1, was added to each well, mixed and the plates incubated for 1 h at 37 °C with 5% CO₂ in the dark. Following incubation, 150 μ l of the medium from each well was transferred to a new 96-well plate and quantification of the formazan dye produced by metabolically active cells was read as absorbance at a wavelength of 420 nm using a scanning multi-well spectrophotometer (Spectra Max 384 Plus, Molecular Devices, USA). The difference in absorbance between the compound-treated cells and the DMSO-treated cells was divided by the absorbance from the DMSO-treated cells and multiplied by 100 to derive the percent inhibition of cell viability values. To derive the cytotoxic IC₅₀ values, confluent HFF and HCT-8 cells were treated with varying concentrations (ranging from 0 to 700 μ M) of compounds. Control cells received varying volumes of DMSO equivalent to the volumes used in the compound-treated cells. The dose–response curves of the means of triplicate assays were generated using GraphPad PRISM software to derive the half maximal inhibitory concentration (IC₅₀) of compounds in HCT-8 and HFF cells.

2.2.3. *C. parvum* growth inhibitory assays

Test compounds that were found not to be toxic to HCT-8 cells at 40 μ M were selected for *in vitro* *C. parvum* growth inhibition tests at 20 μ M concentration. Fresh medium (supplemented RPMI-1640) was added to confluent HCT-8 cells in 96-well plates, followed by inoculation of 4 \times 10⁴ freshly excysted sporozoites to each well. Immediately, test compounds (reconstituted in DMSO) were added to one set of wells at 20 μ M final concentration. Paromomycin reconstituted in distilled sterile water was added to a separate set of wells as a positive control at 800 μ M final concentration (Li et al., 2019). To negative control wells, volumes of DMSO equivalent to the volumes of test compounds used, were added. The cultures were incubated at 37 °C with 5% CO₂, for 72 h after which they were processed for immunofluorescence assay as previously described (Witola et al., 2017). Briefly, medium was removed from the wells by decanting followed by fixing the cells in methanol-acetic acid (9:1) for 2 min at room temperature. The cells were rehydrated and permeabilized by two successive washes with buffer (0.1% Triton X-100, 0.35 M NaCl, 0.13 M Tris-base, pH 7.6) and blocked with 5% normal goat serum, followed by staining with antibody to *C. parvum* (SporoGlo, Waterborn, Inc.) overnight at 4 °C. The stained cells were washed twice with PBS, followed by water, and then imaged with an inverted fluorescence microscope. Fluorescence quantification was done using ImageJ version 1.37v software (NIH). Assays were performed in triplicate and repeated at least thrice.

2.2.4. *T. gondii* growth inhibitory assays

Test compounds that were found not to be toxic to HFF cells at 40 μ M were used to test for inhibitory effect against the growth of *T. gondii* *in vitro*. Fresh supplemented Iscove's modified Dulbecco's medium was added to confluent HFF cells in 96-well plates. About 3500 freshly extracted tachyzoites of *T. gondii* (constitutively expressing YFP) were added to each well, and immediately, test compounds (reconstituted in DMSO) were added to one set of wells at 20 μ M final concentration. Atovaquone (Sigma-Aldrich) reconstituted in DMSO was added to a separate set of wells as a positive control at 0.48 μ M final concentration (Araujo et al., 1991). To negative control wells, volumes of DMSO equivalent to those used for atovaquone and test compounds were added. The cells were incubated at 37 °C with 5% CO₂ for 48 h, after which they were analyzed by fluorescence microscopy to measure parasite YFP fluorescence. Fluorescence quantification was done using ImageJ version 1.37v software (NIH). Assays were performed in triplicate and repeated at least thrice.

2.2.5. Derivation of compound IC₅₀ values against parasites

To derive the IC₅₀ values of the test compounds against *C. parvum*, confluent HCT-8 cells cultures were prepared and infected in 96 well plates as described above, but instead of using a single concentration of test compounds, a series of wells with HCT-8 cells were treated with

varying concentrations (0.0, 2.5, 5.0, 10.0, 20.0, 40.0, 60.0, 80.0, and 100.0 μ M) of test compounds. One set of HCT-8 cells was treated with compounds immediately after infection with *C. parvum* sporozoites, while the other set was treated with compounds 2 h after infection. Control cells received varying volumes of DMSO equivalent to the volumes used in the compound-treated cells. After 72 h of culture, the cells were processed for immunofluorescence assays and analyzed as described above. The dose–response curves of the means of triplicate assays were generated using GraphPad PRISM software to derive the IC₅₀ values.

To derive the IC₅₀ values of test compounds against *T. gondii*, confluent HFF cells were prepared and infected as described above, but instead of using a single concentration of test compounds, the cells were treated with varying concentrations of test compounds (JS-1-09: 0.0, 0.5, 1.0, 2.0, 4.0, 6.0, and 8.0 μ M; JS-2-20, JS-2-35 and JS-2-49: 0.0, 2.5, 10.0, 20.0, 30.0 and 40.0 μ M). One set of HFF cells was treated with compounds immediately after infection with *T. gondii* tachyzoites, while the other set was treated with compounds 2 h after infection. Control cells received varying volumes of DMSO equivalent to the volumes used in the compound-treated cells. After 48 h of culture, the cells were analyzed to quantify parasite fluorescence as described above. The dose–response curves of the means of triplicate assays were generated using GraphPad PRISM software to derive the IC₅₀ values.

2.3. Statistical analyses

Statistical analyses were performed using two-tailed Student's t-test. *P* values of 0.05 or less were considered significant.

3. Results

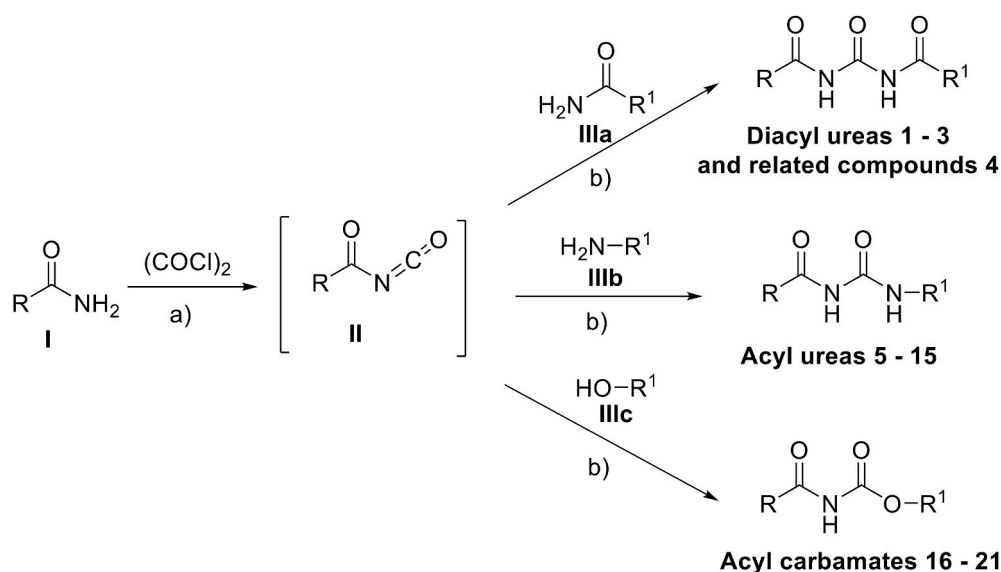
3.1. Chemistry

3.1.1. Synthesis of the test compounds

A series of small molecules belonging to the class of symmetrical and asymmetrical acyl/diacyl ureas and acyl carbamates were synthesized by following the two-step, one-pot synthetic protocol (Scheme 1) (Garcia Hernandez et al., 2017). The respective amides (I) were treated with oxalyl chloride in dry dichloromethane for about 3 h under reflux followed by solvent evaporation. Subsequently, the appropriate nucleophile (III) was quickly added followed by refluxing in dry toluene for approximately 3 h. Upon cooling the reaction mixture to room temperature, the compounds were isolated through concentration and subsequent purification. The final products were obtained in yields ranging from good to excellent, except in cases of difficult purification (Table 1).

3.1.2. Compound screening

The previously reported library of 38 molecules based on the diacyl urea skeleton and related compounds (Garcia Hernandez et al., 2017), was screened *in vitro* for inhibitory activity against *T. gondii* and *C. parvum* parasites. Among all the compounds screened, the symmetrical diacyl urea possessing the *o*-OCH₃ groups showed very high inhibitory activity against *T. gondii* (Table 1). Encouraged by those preliminary results, we employed the synthetic protocol (Scheme 1) with various amines (IIIb) and alcohols (IIIc) as the nucleophile to obtain a small set of acyl ureas (5–15) and acyl carbamates (16–21), respectively (Table 1). Initially, the newly synthesized compounds were evaluated for cytotoxicity against mammalian cells in order to filter out those molecules that are not feasible for further optimization due to toxicity issues. Those molecules, which turned out to be safe at 40 μ M compound concentration, were further tested against *T. gondii* and *C. parvum* parasites at 20 μ M compound concentration. In this manner, four compounds (JS-1-09, JS-2-20, JS-2-35, and JS-2-49) and another molecule (GMG-1-09) were identified to have interesting activity against *T. gondii* and *C. parvum*, respectively (Table 2), and were devoid



Scheme 1. Elaboration of acyl isocyanates (II) obtained from primary amides (I). Reagents and conditions: (a) i. 1.0 mmol of I, dry CH_2Cl_2 , RT, 5 min, ii. 3.0 eq of $(\text{COCl})_2$, reflux 2.5–3 h, iii. RT, *in vacuo* solvent evaporation, (b) i. 1.1–1.25 eq of the appropriate nucleophile (IIIa–c), dry PhMe, reflux, 2.5–3 h, ii. RT, solvent evaporation.

of cytotoxicity against mammalian cell lines.

3.2. Biology

3.2.1. Test compounds without toxicity to host cells, but with anti-parasitic effect *in vitro*

Because *C. parvum* and *T. gondii* were cultured *in vitro* in HCT-8 and HFF cells, respectively, prior to testing the compounds' effects on the parasites, we first determined their effects on the uninfected host cells' viability. We selected 40 μM as the initial concentration at which the compounds were screened for cytotoxicity against the host cells. This selected concentration was two times higher than the targeted initial concentration (20 μM) for screening the compounds against the parasites. Of the total 21 compounds tested, 12 were found to inhibit HCT-8 cell viability by at least 25% and above, while 9 compounds had no inhibitory effect at 40 μM after 48 h of culture (S2 Fig.). The same 12 compounds were found to be toxic (inhibited cell viability by at least 25%) to HFF cells at 40 μM , while the same 9 compounds were tolerable after 48 h of culture without any notable cell viability inhibitory effect that was 25% or above (S3 Fig.).

The 9 compounds that were found to be non-toxic to HCT-8 and HFF cells were selected for testing for anti-*Cryptosporidium* and anti-*Toxoplasma* effect at 20 μM (half the tolerable concentration in host cells). Out of the 9 compounds, one compound (GMG-1-09) was identified to significantly inhibit *C. parvum* growth *in vitro* by about 70%, when compared to the untreated parasites after 48 h of culture (Fig. 1). Paromomycin at 800 μM was used as the inhibitor control and all experimental data were normalized with DMSO-treated wells (0% inhibition) and inhibitor control (100% inhibition) wells as previously reported (Li et al., 2019). On the other hand, we found 4 compounds (JS-1-09, JS-2-20, JS-2-35 and JS-2-49) that had significant inhibitory effect against the growth of *T. gondii* *in vitro* at 20 μM final concentration (Fig. 2). JS-1-09 inhibited growth of *T. gondii* by almost 100%, similar to atovaquone (Araujo et al., 1991) that was used as the positive control drug at 0.5 μM (Fig. 2). Compared to untreated cultures, JS-2-20 and JS-2-35 had about 80%, while JS-2-49 had about 90% inhibitory effect on *T. gondii* growth after 48 h of culture (Fig. 2). The remaining compounds did not show any significant inhibitory effect when compared to the control untreated cultures (Fig. 2).

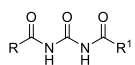
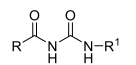
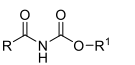
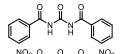
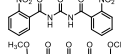
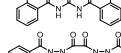
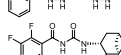
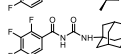
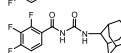
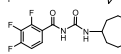
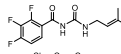
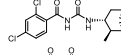
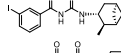
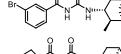
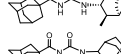
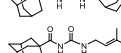
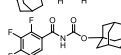
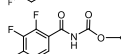
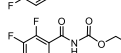
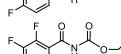
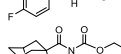
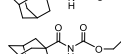
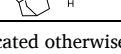

3.2.2. Candidate compounds' cytotoxicity and anti-parasitic IC_{50} concentrations

Compound GMG-1-09 depicted a cytotoxicity IC_{50} concentration of 450.47 μM in HCT-8 cells after 48 h of culture (Table 2). On the other hand, compounds JS-1-09, JS-2-20, JS-2-35 and JS-2-49, had cytotoxicity IC_{50} values that ranged from 59.17 to 65.69 μM (Table 2).

For all compounds that had shown anti-parasitic activity at the initial testing concentration of 20 μM , a secondary screening was performed using varying concentrations and durations of culture to derive the IC_{50} concentrations for the inhibition of parasite proliferation. For each compound, the assays were done in two formats: (1) by adding the compound to the host cells culture immediately after infecting them with parasites, and (2) by adding the compounds to the cells 2 h post-infection. This was meant to assess the effect of the compounds when parasites were exposed to the compounds prior to, and after infecting the host cells. When the cultures were analyzed at 48 h post-infection, compound GMG-1-09 was found to have a significant ($P < 0.05$) concentration-dependent effect of inhibiting proliferation of intracellular *C. parvum* merozoites in HCT-8 cells starting at 15 μM when compared to the control infected cultures without compound treatment (Fig. 3). When GMG-1-09 was added to the cultures 2 h post-infection, a similar trend of concentration-dependent reduction in parasite growth, but with a slight decrease (though insignificant) in compound efficacy relative to treating at the time of infection was observed (Fig. 3). By using GraphPad PRISM software, the half maximal inhibitory concentration (IC_{50}) value (32.24 μM) of GMG-1-09 for *C. parvum* *in vitro* was derived from the dose–response curve. The anti-*Cryptosporidium* IC_{50} of GMG-1-09 was approximately 14-fold lower than its cytotoxicity IC_{50} , indicating that this compound can be considered as non-toxic to the host cells at its effective anti-parasitic concentration.

When titrated at varying concentrations, compounds JS-1-09, JS-2-49, JS-2-35, and JS-2-20 all reduced *T. gondii* growth in a concentration-dependent manner (Fig. 4A–D). There was no significant difference in the compounds' effect between adding the compound to culture immediately or 2 h post-infection (Fig. 4A–D). The anti-*Toxoplasma* IC_{50} value of JS-1-09 was approximately 53-fold lower than its corresponding cytotoxicity IC_{50} value (Table 2). On the other hand, the antiparasitic activities of JS-2-20, JS-2-35 and JS-2-49 were only 5 to 6 times lower than their corresponding cytotoxicity IC_{50} values (Table 2). Those data imply that compound JS-1-09 was effective against *T. gondii* at a concentration that was not toxic to mammalian host cells with a wide safety

Table 1Reported diacyl ureas, acyl ureas and acyl carbamates with their overall yields, ClogP values, and IC₅₀ indices against *T. gondii* and *C. parvum* parasites.

Compound		Starting Material I	Nucleophile III	Final Product	Yield ^a	ClogP ^g	IC ₅₀ (μM)	
Code	No						<i>T. gondii</i>	<i>C. parvum</i>
<div style="display: flex; justify-content: space-around; align-items: center;"> <div style="text-align: center;">  <p>Diacyl ureas 1-3 and related compounds (4)</p> </div> <div style="text-align: center;">  <p>Acyl ureas 5-15</p> </div> <div style="text-align: center;">  <p>Acyl carbamates 16-21</p> </div> </div>								
JS-1-07	1	a	a		89 ^{b,c}	2.64	NA ^h	NA
JS-1-11	2	b	b		70 ^{c,d}	0.90	NA	NA
JS-1-09	3	c	c		88 ^{b,c}	2.71	1.21	NA
JS-1-37	4	d	d		77 ^{b,c}	-0.86	NA	NA
JS-2-11	5	e	e		59	5.31	NT ⁱ	NT
JS-2-14	6	e	f		49 ^e	4.11	NT	NT
JS-2-34	7	e	g		63	5.15	NT	NT
JS-2-36	8	e	h		85	4.60	NT	NT
JS-2-20	9	e	i		34 ^e	5.18	10.92	NA
JS-2-10	10	f	e		66	6.00	NT	NT
JS-2-16	11	g	e		70 ^f	6.46	NT	NT
JS-2-17	12	h	e		66	6.20	NT	NT
AGH-1-09	13	i	e		58	5.89	NT	NT
GMG-1-11	14	i	g		60 ^e	5.73	NT	NT
JS-2-21	15	i	i		84	5.76	NT	NT
JS-2-49	16	e	j		81	4.16	12.09	NA
JS-2-35	17	e	k		98	5.20	10.49	NA
AGH-1-08	18	e	l		60	5.23	NT	NT
GMG-1-10	19	e	m		45 ^e	5.23	NT	NT
GMG-1-08	20	i	l		31 ^e	4.92	NA	NA
GMG-1-09	21	i	m		29 ^e	4.92	NA	32.24

^a Yield reported after purification by flash chromatography on silica (unless indicated otherwise).^b Isolated pure crude material.^c Compound reported previously (Garcia Hernandez et al., 2017).^d After purification by crystallization from methanol.^e Difficult purification by column chromatography hence the low yield.^f After purification by recrystallization from hexane : ethyl acetate.^g Calculated with ChemDraw Professional 15.1.^h NA = not active.ⁱ NT = not tested against parasites due to apparent cytotoxicity against mammalian cells.

margin, whereas the remaining three compounds showed barely appreciable selectivity indices.

4. Discussion

Herein, we present results showing a series of small molecules bearing the acyl and diacyl urea as well as acyl carbamate scaffold that possess interesting antiprotozoal activity at low micromolar concentrations. They also show appreciable safety margins in human host cells.

Prior to testing the compounds for antiparasitic activity, we tested their toxicity in human cell lines HCT-8 and HFF, which were used for culturing *C. parvum* and *T. gondii*, respectively. Those molecules that were tolerable at high micromolar concentrations (IC₅₀ > 40 μM) were subsequently tested for anti-parasitic activity. Importantly, we found that the antiparasitic IC₅₀ values for some of the compounds with antiparasitic efficacy were much lower than their corresponding cytotoxicity IC₅₀ values, underscoring that they are effective against the parasites at concentrations that are not toxic to host cells. We observed

Table 2

Cytotoxicity and antiparasitic IC₅₀ values for test compounds along with calculated selectivity indices.

Compound	Cytotoxicity IC ₅₀ (μM)	Anti-parasitic IC ₅₀ (μM)	Selectivity index (SI) ^d
JS-1-09	64.05 ^a	1.21 ^b	52.9
JS-2-20	62.65 ^a	10.92 ^b	5.7
JS-2-35	59.17 ^a	10.49 ^b	5.6
JS-2-49	65.49 ^a	12.09 ^b	5.4
GMG-1-09	450.47 ^{**}	32.24 ^c	14.0

^a Cytotoxicity IC₅₀ value against human foreskin fibroblasts (HFF); ^{**}Cytotoxicity IC₅₀ value against human ileocecal adenocarcinoma (HCT-8) cells.

^b Anti-*Toxoplasma* IC₅₀.

^c Anti-*Cryptosporidium* IC₅₀.

^d Selectivity Index (SI) = Cytotoxicity IC₅₀/Anti-parasitic IC₅₀.

that atovaquone, a positive control drug that was used at 0.5 μM concentration, almost completely inhibited *T. gondii* growth, similar to the effect of the test compound JS-1-09 at 8 μM. While atovaquone has been shown to be toxic to human host cells *in vitro* at a concentration that is 10-fold higher than its effective parasite inhibitory concentration (Araujo et al., 1991), we found that JS-1-09 had an anti-*Toxoplasma* IC₅₀ concentration that was 53-fold lower than its cytotoxicity IC₅₀ value, suggesting that it may be efficacious with a wider safety margin. Likewise, other potent compounds JS-2-20, JS-2-35 and JS-2-49 showed potency against *T. gondii* at about 5-6-fold lower concentrations than their cytotoxicity IC₅₀ concentrations. In treating *T. gondii* infections, this would be important in circumventing the problems of toxicity and hypersensitivity that are associated with currently licensed drugs for human treatment (McLeod et al., 2006; Rajapakse et al., 2013; Montazeri et al., 2015). The small number of compounds tested against the two parasites does not necessarily allow outlining clear structure-activity relationship for this set of compounds. While JS-1-09 is structurally divergent and represents symmetrical diacyl urea, the other 3 compounds (JS-2-20, JS-2-35 and JS-2-49) that also showed efficacy against *T. gondii* represent the acyl urea (JS-2-20) and acyl carbamate (JS-2-35 and JS-2-49) scaffold. JS-1-09 can be potentially considered as a remote derivative of QQ-437 (S1 Fig.), whereas JS-2-35 and JS-2-49 can be viewed as acyl carbamate derivatives of the antimycobacterial lead AU1235 (Fig. 5) (Grzegorzewicz et al., 2012). Interestingly, JS-2-20 can also be regarded as the acyl urea combination of the 1,2,3-trifluorophenyl moiety (left-hand side) of AU1235 and the geranyl chain (right-hand side) of another antituberculosis agent SQ109 (Protopopova et al., 2005), which is currently in phase II of clinical trials

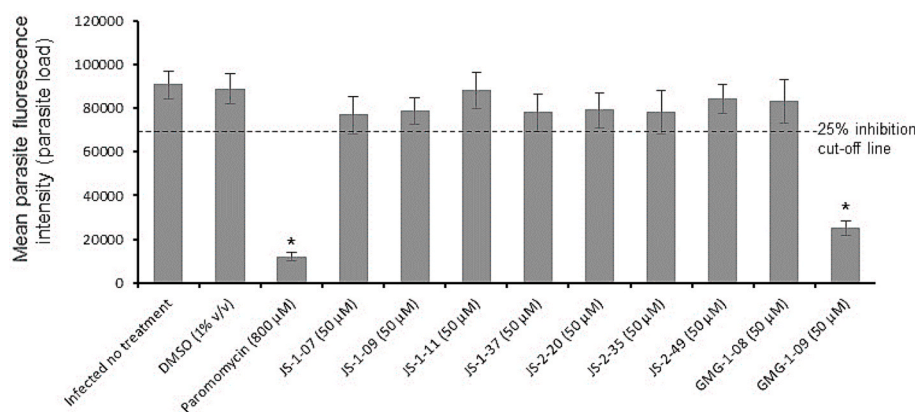


Fig. 1. Analysis of the effects of test compounds on the growth of *Cryptosporidium parvum* in human ileocecal adenocarcinoma (HCT-8) cells *in vitro*. Equal amounts of freshly excysted sporozoites of *C. parvum* were inoculated into HCT-8 cells in culture and immediately treated with 20 μM of compound JS-1-07, JS-1-09, JS-1-11, JS-1-37, JS-2-20, JS-2-35, JS-2-49, GMG-1-08 or GMG-1-09. Infected cells without compound-treatment, but with equivalent amount of DMSO to that used in compound-treated cells (1% v/v) were set as negative controls. Positive control cultures were treated with paromomycin (800 μM). After 72 h the cultures were analyzed for parasite proliferation by immunofluorescence assays. The fluorescence generated by *C. parvum* was quantified and is shown on the Y-axis representing the parasite load. The data shown represent the means from three independent experiments with standard error bars, and levels of statistical significance depicted by asterisks (*, $P < 0.05$).

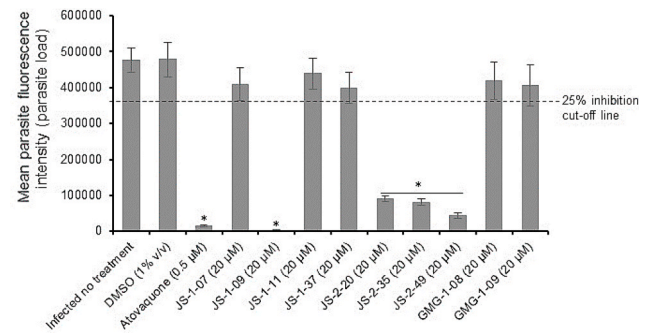


Fig. 2. Analysis of the effects of test compounds on the growth of *T. gondii* *in vitro*. Equal amounts (500) of *T. gondii* tachyzoites constitutively expressing yellow fluorescent protein (YFP) were used to infect confluent monolayers of human foreskin fibroblasts (HFF) and immediately treated with 20 μM of compound JS-1-07, JS-1-09, JS-1-11, JS-1-37, JS-2-20, JS-2-35, JS-2-49, GMG-1-08 or GMG-1-09. Infected cells without compound-treatment, but with DMSO equivalent to volume used in compound-treated cells (1% v/v) were set as negative controls. Positive control cultures were treated with atovaquone (0.5 μM). After 48 h, the cultures were analyzed for parasite proliferation by measuring the parasite YFP fluorescence by fluorescence microscopy. The fluorescence generated by *T. gondii* was quantified and is shown on the Y-axis representing the parasite load. The data shown represent the means from three independent experiments with standard error bars, and levels of statistical significance depicted by asterisks (*, $P < 0.05$).

(Fig. 5) (NIH and U.S. National Library of Medicine, 1785). Current medicines against *T. gondii* infections are not effective against the encysted bradyzoite stage of the parasite, and thus cannot eliminate the infection in chronically infected individuals. Therefore, future studies will be directed at assessing the efficacy of these candidate compounds and their derivatives against both the tachyzoite and bradyzoite stages of *T. gondii* *in vivo*.

Among all the compounds tested, only GMG-1-09 had *in vitro* efficacy against *C. parvum* with an anti-*Cryptosporidium* IC₅₀ concentration that was 14-fold lower than its cytotoxicity IC₅₀ concentration in a human intestinal cell line (HCT-8). We used paromomycin as a positive control that has an anti-*Cryptosporidium* IC₅₀ of 450 μM (Li et al., 2019) and has been shown to be non-toxic to human cells at concentrations higher than 1000 μM (Gargala et al., 2000; Downey et al., 2008). Comparatively, compound GMG-1-09 was efficacious against *C. parvum* at a much lower concentration (IC₅₀ = 32.34 μM) than paromomycin. Interestingly, while GMG-1-09 had activity against *C. parvum*, it was not potent against *T. gondii*. Noteworthy, GMG-1-09 has a chemical structure, which does

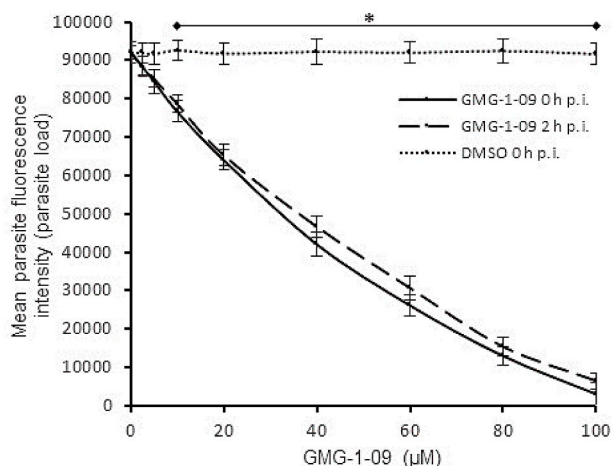


Fig. 3. Effect of varying concentrations of compound GMG-1-09 on the growth of *Cryptosporidium parvum* in HCT-8 cells. Equal amounts of freshly excysted sporozoites of *C. parvum* were inoculated into HCT-8 cells in culture and varying concentrations of GMG-1-09 added at the time of infection (solid line) or at 2 h post-infection (p.i.) (dashed line). Control infected cells (dotted line) were treated immediately p.i. with volumes of DMSO equivalent to those used in the compound-treated cultures. The cells were analyzed for parasite infectivity and proliferation by an immunofluorescence assay after 72 h of culture. The fluorescence generated by intracellular *C. parvum* merozoites was quantified and is shown on the Y-axis representing the parasite load. The data shown represent means of three independent experiments with standard error bars and levels of statistical significance between groups indicated by asterisk (*, $P < 0.05$).

not contain the aromatic moiety that is observed in the structures of the 4 compounds (JS-1-09, JS-2-20, JS-2-35 and JS-2-49) active against *T. gondii*. In addition to that, GMG-1-09 could also be viewed as a carbamate analog of SQ109 that possesses *Z*-geometry of the double bond in the geranyl portion (which is opposite to the *E*-geometry present in SQ109). Even if *T. gondii* and *C. parvum* are both apicomplexan coccidian protozoans, they differ considerably at metabolic level, which in turn could explain, to some extent, the observed difference in anti-protozoal activity of the tested compounds. Based on the completed and annotated genome sequence of *Cryptosporidium*, it is evident that, while the parasite lacks genes for conventional molecular drug targets found in other important protozoan parasites, it possesses several genes encoding plant-like and bacterial-like enzymes that catalyze potentially essential biosynthetic and metabolic pathways (Li et al., 2019; Abrahamsen et al., 2004). Therefore, it is possible that the compounds that we found to have activity against *T. gondii* but not *C. parvum*, could be targeting specific essential metabolic pathways that are present in *T. gondii* but absent in *C. parvum*. Likewise, compound GMG-1-09 that had potency against *C. parvum*, but not *T. gondii*, possibly targets an essential pathway in *C. parvum* that is absent or different in *T. gondii*.

5. Conclusions

In conclusion, our study unveils a series of novel synthetic diacyl/acyl urea and acyl carbamate scaffold-based small molecules with potent activity against *T. gondii* and *C. parvum* at relatively much lower concentrations compared to their cytotoxic levels in human host cells. Through this exploratory study, we identified at least two hit compounds that showed appreciable activity and selectivity against *T. gondii* and *C. parvum*, respectively. Given the simple structure of the active

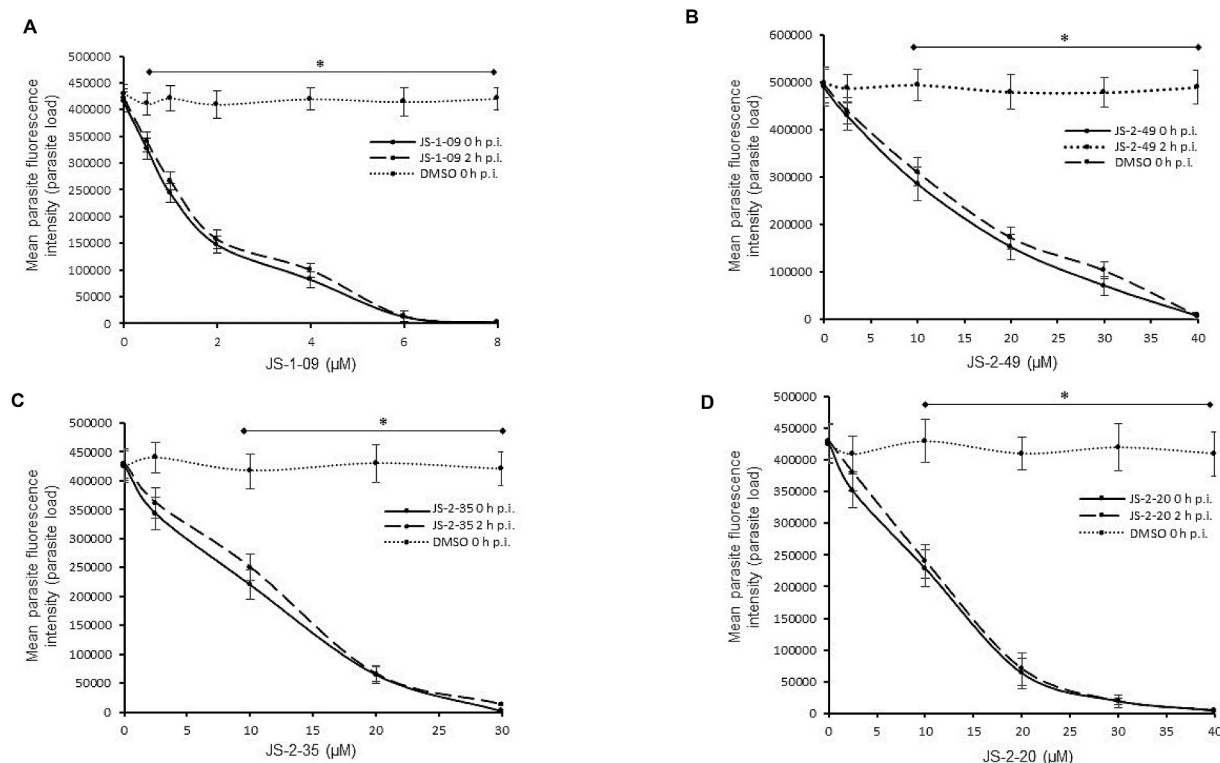


Fig. 4. Effect of varying concentrations of compounds on the growth of *Toxoplasma gondii* in human foreskin fibroblasts (HFF) cells. Equal amounts (500) of *T. gondii* tachyzoites constitutively expressing yellow fluorescent protein (YFP) were used to infect confluent monolayers of HFF cells and immediately (solid lines) or 2 h (dashed lines) after infection treated with varying concentrations of compound JS-1-09 (A), JS-2-49 (B), JS-2-35 (C), or JS-2-20 (D). Infected cells without compound-treatment, but with DMSO equivalent to volumes used in compound-treated cells were set as negative controls (DMSO h p.i.). After 48 h, the cultures were analyzed for parasite proliferation by measuring the parasite YFP fluorescence by fluorescence microscopy. The fluorescence generated by *T. gondii* was quantified and is shown on the Y-axis representing the parasite load. The data shown represent the means from three independent experiments with standard error bars, and levels of statistical significance depicted by asterisks (*, $P < 0.05$).

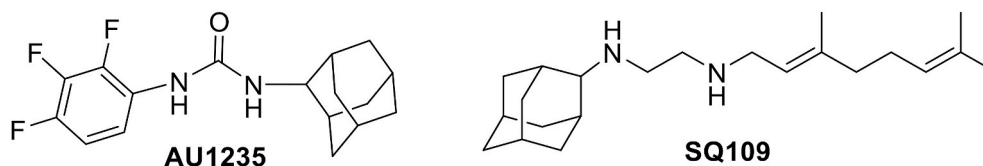


Fig. 5. Structures of the potent antitubercular agents: AU1235 and SQ109.

compounds and good potential for chemical diversification, the identified molecules present a feasible starting point for future medicinal chemistry structure optimization in search of the much-needed safe and effective anti-protozoal drugs.

Declaration of competing interest

The authors declare that they have no known competing financial interests or personal relationships that could have appeared to influence the work reported in this paper.

Acknowledgements

This study was supported in part by funds from the University of Illinois at Urbana-Champaign, USA, to WHW. GMG, AGH, and JS acknowledge Chicago State University (CSU) COP and CSU CTRE (Seed Grant) for generous financial support of this project. The unlimited access to the NMR facility (JEOL 400) in the Department of Chemistry at CSU is acknowledged. Mr. Daniel Pietryla is acknowledged for providing technical assistance in the laboratory. JS wishes to acknowledge MBKU COP for startup funds and faculty travel stipend to present this work at conferences.

Appendix A. Supplementary data

Supplementary data to this article can be found online at <https://doi.org/10.1016/j.ijpddr.2020.08.006>.

References

- Abrahamsen, M.S., Templeton, T.J., Enomoto, S., Abrahante, J.E., Zhu, G., Lancto, C.A., Deng, M., Liu, C., Widmer, G., Tzipori, S., Buck, G.A., Xu, P., Bankier, A.T., Dear, P. H., Konfortov, B.A., Spriggs, H.F., Iyer, L., Anantharaman, V., Aravind, L., Kapur, V., 2004. Complete genome sequence of apicomplexan. *C. parvum*. *Science*. 304, 441–445. <https://doi.org/10.1126/science.1094786>.
- Abubakar, I., Aliyu, S.H., Arumugam, C., Usman, N.K., Hunter, P.R., 2007. Treatment of cryptosporidiosis in immunocompromised individuals: systematic review and meta-analysis. *Br. J. Clin. Pharmacol.* 63, 387–393. <https://doi.org/10.1111/j.1365-2125.2007.02873.x>.
- Alday, P.H., Doggett, J.S., 2017. Drugs in development for toxoplasmosis: advances, challenges, and current status. *Drug Des. Dev. Ther.* 11, 273–293.
- Araujo, F.G., Huskinson, J., Remington, J.S., 1991. Remarkable in vitro and in vivo activities of the hydroxynaphthoquinone 566C80 against tachyzoites and tissue cysts of *Toxoplasma gondii*. *Antimicrob. Agents Chemother.* 35, 293–299.
- Arrowood, M.J., Sterling, C.R., 1987. Isolation of *Cryptosporidium* oocysts and sporozoites using discontinuous sucrose and isopycnic Percoll gradients. *J. Parasitol.* 73, 314–319.
- Boyom, F.F., Fokou, P.V.T., Tchokouaha, L.R.Y., Spangenberg, T., Mfopa, A.N., Kouipou, R.M.T., Mbouna, C.J., Donkeng Donfack, V.F., Zollo, P.H.A., 2014. Repurposing the open access malaria box to discover potent inhibitors of *Toxoplasma gondii* and *Entamoeba histolytica*. *Antimicrob. Agents Chemother.* 58, 5848–5854. <https://doi.org/10.1128/AAC.02541-14>.
- Centers for Disease Control and Prevention Cdc. Parasites – toxoplasmosis: epidemiology & risk factors. <https://www.cdc.gov/parasites/toxoplasmosis/epi.html>. (Accessed 9 April 2020).
- Centers for Disease Control and Prevention Cdc. Parasites – toxoplasmosis. <https://www.cdc.gov/parasites/toxoplasmosis/index.html>. (Accessed 9 April 2020).
- Chalmers, R.M., 2014. *Cryptosporidium*. In: Percival, S.L., Williams, D.W., Gray, N.F., Yates, M.V., Chalmers, R.M. (Eds.), *Microbiology of Waterborne Diseases*, second ed. Academic Press, pp. 287–326.
- Checkley, W., White, A.C., Jaganath, D., Arrowood, M.J., Chalmers, R.M., Chen, X.M., Fayer, R., Griffiths, J.K., Guerrant, R.L., Hedstrom, L., Huston, C.D., Kotloff, K.L., Kang, G., Mead, J.R., Miller, M., Petri Jr., W.A., Priest, J.W., Roos, D.S., Striepen, B., Thompson, R.C., Ward, H.D., Van Voorhis, W.A., Xiao, L., Zhu, G., Houpt, E.R., 2015. A review of the global burden, novel diagnostics, therapeutics, and vaccine targets for *Cryptosporidium*. *Lancet Infect. Dis.* 15, 85–94. [https://doi.org/10.1016/S1473-3099\(14\)70772-8](https://doi.org/10.1016/S1473-3099(14)70772-8).
- Current, W.L., 1992. Techniques and laboratory maintenance of *Cryptosporidium*, p 44–77. In: Dubey, J.P., Speer, C.A., Fayer, R. (Eds.), *Cryptosporidiosis of Man and Animals*. CRC Press, pp. 44–77.
- Deng, H., Huang, X., Jin, C., Jin, C.M., Quan, Z.S., 2020. Synthesis, in vitro and in vivo biological evaluation of dihydroartemisinin derivatives with potential anti-*Toxoplasma gondii* agents. *Bioorg. Chem.* 94, 103467.
- Downey, A.S., Chong, C.R., Graczyk, T.K., Sullivan, D.J., 2008. Efficacy of pyriminium pamoate against *Cryptosporidium parvum* infection in vitro and in a neonatal mouse model. *Antimicrob. Agents Chemother.* 52, 3106–3112. <https://doi.org/10.1128/AAC.00207-08>.
- Fomovska, A., Huang, Q., El Bissati, K., Mui, E.J., Witola, W.H., Cheng, G., Zhou, Y., Somerville, C., Roberts, C.W., Bettis, S., Prigge, S.T., Afanador, G.A., Hickman, M. R., Lee, P.J., Leed, S.E., Auschwitz, J.M., Pieroni, M., Stec, J., Muench, S.P., Rice, D. W., Kozikowski, A.P., McLeod, R., 2012. Unique parasite secretory pathway disrupted by novel hydroxybenzamides. *Antimicrob. Agents Chemother.* 56, 2666–2682.
- Furtado, J.M., Smith, J.R., Belfort Jr., R., Gattey, D., Winthrop, K.L., 2011. Toxoplasmosis: a global threat. *J. Global Infect. Dis.* 3, 281–284. <https://doi.org/10.4103/0974-777X.83536>.
- Garcia Hernandez, A., Grooms, G.M., El-Alfy, A.T., Stec, J., 2017. Convenient one-pot two-step synthesis of symmetrical and unsymmetrical diacyl ureas, acyl urea/ carbamate/thiocarbamate derivatives, and related compounds. *Synthesis* 49, 2163–2176. <https://doi.org/10.1055/s-0036-1588724>.
- Gargala, G., Delaunay, A., Li, X., Brasseur, P., Favennec, L., Ballet, J.J., 2000. Efficacy of nitazoxanide, tizoxanide and tizoxanide glucuronide against *Cryptosporidium parvum* development in sporozoite-infected HCT-8 enterocytic cells. *J. Antimicrob. Chemother.* 46, 57–60.
- Grzegorzewicz, A.E., Pham, H., Gundi, V.A., Scherman, M.S., North, E.J., Hess, T., Jones, V., Gruppo, V., Born, S.E., Korduláková, J., Chavadi, S.S., Morisseau, C., Lenaerts, A.J., Lee, R.E., McNeil, M.R., Jackson, M., 2012. Inhibition of mycolic acid transport across the *Mycobacterium tuberculosis* plasma membrane. *Nat. Chem. Biol.* 8, 334–341. <https://doi.org/10.1038/nchembio.794>.
- Gubbels, M.J., Li, C., Striepen, B., 2003. High-throughput growth assay for *Toxoplasma gondii* using yellow fluorescent protein. *Antimicrob. Agents Chemother.* 47, 309–316.
- Guo, H.Y., Jin, C., Zhang, H.M., Jin, C.M., Shen, O.K., Quan, Z.S., 2019. Synthesis and biological evaluation of (+)-Usnic acid derivatives as potential anti-*Toxoplasma gondii* agents. *J. Agric. Food Chem.* 67, 9630–9642. <https://doi.org/10.1021/acs.jafc.9b02173>.
- Kochanowsky, J.A., Koshy, A.A., 2018. *Toxoplasma gondii*. *Curr. Biol.* 28, R770–R771.
- Krivogorsky, B., Nelson, A.C., Douglas, K.A., Grundt, P., 2013. Trypanthrin derivatives as *Toxoplasma gondii* inhibitors – structure-activity-relationship of the 6-position. *Bioorg. Med. Chem. Lett* 23, 1032–1035.
- Kuhlenschmidt, T.B., Rutaganira, F.U., Long, S., Tang, K., Shokat, K.M., Kuhlenschmidt, M.S., Sibley, L.D., 2016. Inhibition of Calcium-Dependent Protein Kinase 1 (CDPK1) in vitro by pyrazolopyrimidine derivatives does not correlate with sensitivity of *Cryptosporidium parvum* growth in cell culture. *Antimicrob. Agents Chemother.* 60, 570–579. <https://doi.org/10.1128/AAC.01915-15>.
- Li, K., Nader, S.M., Zhang, X., Ray, B.C., Kim, C.Y., Das, A., Witola, W.H., 2019. Novel lactate dehydrogenase inhibitors with in vivo efficacy against *Cryptosporidium parvum*. *PLoS Pathog.* 15, e1007953.
- Luan, T., Jin, C., Jin, C.M., Gong, G.H., Quan, Z.S., 2019. Synthesis and biological evaluation of ursolic acid derivatives bearing triazole moieties as potential anti-*Toxoplasma gondii* agents. *J. Enzym. Inhib. Med. Chem.* 344, 761–772. <https://doi.org/10.1080/14756366.2019.1584622>.
- Martins-Duarte, É.S., Jones, S.M., Gilbert, I.H., Atella, G.C., de Souza, W., Vommaro, R. C., 2009. Thiolactomycin analogues as potential anti-*Toxoplasma gondii* agents. *Parasitol. Int.* 58, 411–415.
- Mboera, L.E.G., Kishamawe, C., Kimario, E., Rumisha, S.F., 2019. Mortality patterns of toxoplasmosis and its comorbidities in Tanzania: a 10-year retrospective hospital-based survey. *Front. Public Health* 7, 25. <https://doi.org/10.3389/fpubh.2019.00025>.
- McLeod, R., Khan, A., Nobel, G., Latkany, P., Jalbrzikowski, J., Boyer, K., 2006. Severe sulfadiazine hypersensitivity in a child with reactivated congenital toxoplasmic chorioretinitis. *Pediatr. Infect. Dis. J.* 25, 270–272.
- Montazeri, M., Daryani, A., Ebrahimzadeh, M., Ahmadvan, E., Sharif, M., Sarvi, S., 2015. Effect of propranolol alone and in combination with pyrimethamine on acute murine toxoplasmosis. *Jundishapur J. Microbiol.* 8, e22572 <https://doi.org/10.5812/jjm.22572>.
- Nih, U.S. National Library of Medicine. <https://clinicaltrials.gov/ct2/show/NCT01785186>. (Accessed 9 April 2020).

- Protopopova, M., Hanrahan, C., Nikonenko, B., Samala, R., Chen, P., Gearhart, J., Einck, L., Nacy, C.A., 2005. Identification of a new antitubercular drug candidate, SQ109, from a combinatorial library of 1,2-ethylenediamines. *J. Antimicrob. Chemother.* 56, 968–974. <https://doi.org/10.1093/jac/dki319>.
- Rajapakse, S., Chrisan Shivanthan, M., Samaranayake, N., Rodrigo, C., Deepika Fernando, S., 2013. Antibiotics for human toxoplasmosis: asystematic review of randomized trials. *Pathog. Glob. Health* 107, 162–169.
- Witola, W.H., Zhang, X., Kim, C.Y., 2017. Targeted gene knockdown validates the essential role of lactate dehydrogenase in *Cryptosporidium parvum*. *Int. J. Parasitol.* 47, 867–874. <https://doi.org/10.1016/j.ijpara.2017.05.002>.
- Zhang, H.B., Shen, Q.K., Wang, H., Jin, C., Jin, C.H., Quan, Z.S., 2018. Synthesis and evaluation of novel arctigenin derivatives as potential anti-*Toxoplasma gondii* agents. *Eur. J. Med. Chem.* 158, 414–427.
- Zhou, Y., Fomovska, A., Muench, S., Lai, B.S., Mui, E., McLeod, R., 2014. Spiroindolone that inhibits PfATPase4 is a potent, cidal inhibitor of *Toxoplasma gondii* tachyzoites in vitro and in vivo. *Antimicrob. Agents Chemother.* 58, 1789–1792.